Interferometric correlogram-space analysis

Oleg V. Poliannikov* Mark E. Willis†

April 26, 2010

Abstract

Seismic interferometry is a method of obtaining a virtual shot gather from a collection of physical shot gathers. The set of traces corresponding to two common receiver gathers from many physical shots is used to synthesize a virtual shot located at one of the receivers and a virtual receiver at the other. An estimate of a Green's function between these two receivers is obtained by first cross-correlating corresponding pairs of traces from each of the shots and then stacking the resulting cross-correlograms. In this paper, we study the structure of cross-correlograms obtained from a VSP acquisition geometry using surface sources and down-hole receivers. The model is purely acoustic and contains flat or dipping layers and/or point inclusions that act as diffractors. Results of a semblance-based moveout scan of the cross-correlograms are used to identify the potential geometry of the reflectors. This new information allows improvements in the quality of the trace at the virtual receiver by either rejecting those moveouts or enhancing them before the stack is performed.

1 Introduction

The ultimate goal of many seismic applications is to create an image of a portion of the subsurface. While one usually has greater freedom placing receivers, locating sources close to the target image area is often technologically impractical. Seismic interferometry is a method of redatuming (or numerically moving) physical shots to be as if they were located at the receiver locations. Of course, using reciprocity we can switch this to also allow redatuming receivers to the shot locations. A potential benefit of redatuming surface sources to the receivers is that overburden effects between the physical source and the virtual source will be (approximately) removed. This can reduce the distortions caused by complicated near surface velocity issues, for example.

The set of traces corresponding to two common receiver gathers (CRG) from many physical shots is used to synthesize a virtual shot located at one of the

*Earth Resources Laboratory, Department of Earth, Atmospheric and Planetary Sciences, Massachusetts Institute of Technology, Building 54-521A, 77 Massachusetts Avenue, Cambridge, MA 02139-4307. Email: poliann@mit.edu

†ConocoPhillips Company, 600 N. Dairy Ashford, Houston TX 77079

receivers and a virtual receiver at the other. An estimate of the Green's function between these two receivers is obtained by first cross-correlating corresponding pairs of traces from each of the shots and then stacking the resulting cross-correlograms [1]. One of the receivers is labeled as the virtual source (VS), and the other one becomes a virtual receiver (VR). This technique is used in ocean bottom cable acquisition geometries to create virtual shots on the ocean's bottom. In VSP geometries the surface shots can be redatumed to the borehole receiver positions and vice versa [2, 3, 4]. The details of the theory for constructing an interferometrically redatumed trace are well-known [5, 6, 7, 8, 9], but will be summarized below.

The accuracy of the redatumed trace is subject to various requirements, including that the source illumination needs to be along a continuous enclosed contour around the medium. Some artifacts in the redatumed trace are expected since this condition is not met in most applications. If there is a significant gap in source coverage the edge of the gap will introduce phantom events which may completely obscure the actual reflections. Even if the source illumination around the medium is angularly complete but is spatially undersampled (e.g., by having a source spacing larger than a wavelength) then ringing, aliased noise is introduced into the stack [10].

The redatumed, virtual trace created at the VR will contain the reflection events that would be expected from formation boundaries illuminated by a source located at the VS. Each valid reflection in the virtual trace will come from a stationary phase point in its corresponding cross-correlogram. With proper source illumination it is hoped that all other events in the cross-correlogram will not be aligned and will stack out.

Conventional "brute" stacking of the cross-correlogram to create the redatumed trace ignores the geometric moveout of events and attempts to keep only the contributions from the stationary phase points. We would like to use the moveout information to first characterize all of the events and then selectively enhance the desired events and remove the undesirable events and artifacts. We view the correlogram as a basic building block for performing interferometry and propose that it should be analyzed and preprocessed when necessary before stacking. We propose a cross-correlogram moveout analysis that will allow events to be identified and then modified so that the quality of the redatumed trace is improved.

2 Mathematical foundations

2.1 Model setup and classical interferometry

Our model is a two-dimensional acoustic medium representing a VSP experiment, although the ideas and conclusions are general. We place sources, $\boldsymbol{x}_{\mathrm{s}}$, on the surface $\mathscr{S}$ and receivers, $\boldsymbol{x}_{\mathrm{r}}$, down in a vertical borehole.

The formations we consider are point diffractors and parallel, linear reflectors. As shown in Figure 1, diffractors are geometrically specified by their co-

ordinates $(x_{\rm d}, z_{\rm d})$, while the position of a reflector can be described by a single point (x_ℓ, z_ℓ) with a dip θ_ℓ.

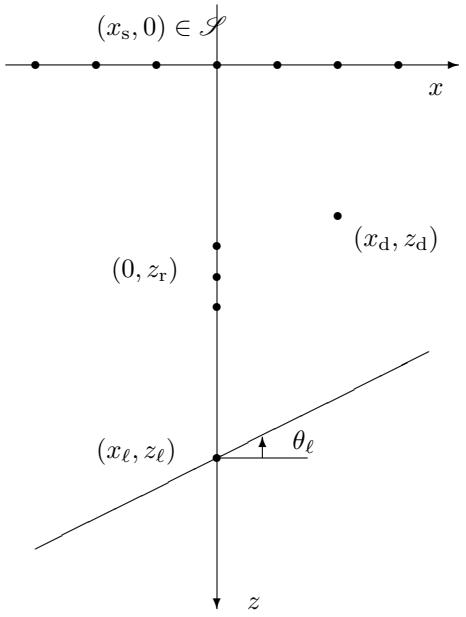

Figure 1: VSP acquisition geometry and associated notation. Surface shot locations have coordinates $(x_{\rm s}, 0)$, receivers are located in a vertical borehole: $(0, z_{\rm r})$. Point diffractors are defined by their coordinates $(x_{\rm d}, z_{\rm d})$, and reflectors are given by a "base point" (x_ℓ, z_ℓ) and dip θ_ℓ.

We want to redatum all surface shots at $\mathscr{S}$ to two receiver locations $\boldsymbol{x}_{\rm r,1}$ and $\boldsymbol{x}_{\rm r,2}$ in the borehole. The redatuming process is based on Rayleigh reciprocity theorem [11, 9, 12]. If $\mathscr{S}$ is a closed continuous curve (or surface in 3D) surrounding the medium then

$$\underbrace{G\left(\boldsymbol{x}_{\rm r,1}, \boldsymbol{x}_{\rm r,2}, -t\right)}_{\text{anticausal GF}} + \underbrace{G\big(\overbrace{\boldsymbol{x}_{\rm r,1}}^{\text{VS}}, \overbrace{\boldsymbol{x}_{\rm r,2}}^{\text{VR}}, t\big)}_{\text{causal GF}} \propto \underbrace{\oint\limits_{\mathscr{S}}}_{\text{stacking}} \underbrace{\overbrace{G\left(\boldsymbol{x}_{\rm s}, \boldsymbol{x}_{\rm r,1}, -t\right)}^{\text{CRG}_1} \star \overbrace{G\left(\boldsymbol{x}_{\rm s}, \boldsymbol{x}_{\rm r,2}, t\right)}^{\text{CRG}_2}}_{\text{correlogram}} d\boldsymbol{x}_{\rm s}, \tag{1}$$

Figure 2 shows a specific flat layer model with two reflectors. Figures 3a and 3b show the two common receiver gathers using all of the surface sources shooting into the two subsurface receivers. Corresponding traces in the two

common receiver gathers are cross-correlated. The cross-correlogram is shown in Figure 3c. Here we display only the positive lags since we are interested in reconstructing the causal part of the Green's function. The traces in the correlogram are summed together to produce a stack, shown in Figure 3d. We have applied some weighting to the traces in the stack to mitigate edge effects as will be described in section on Filtering Correlograms below.

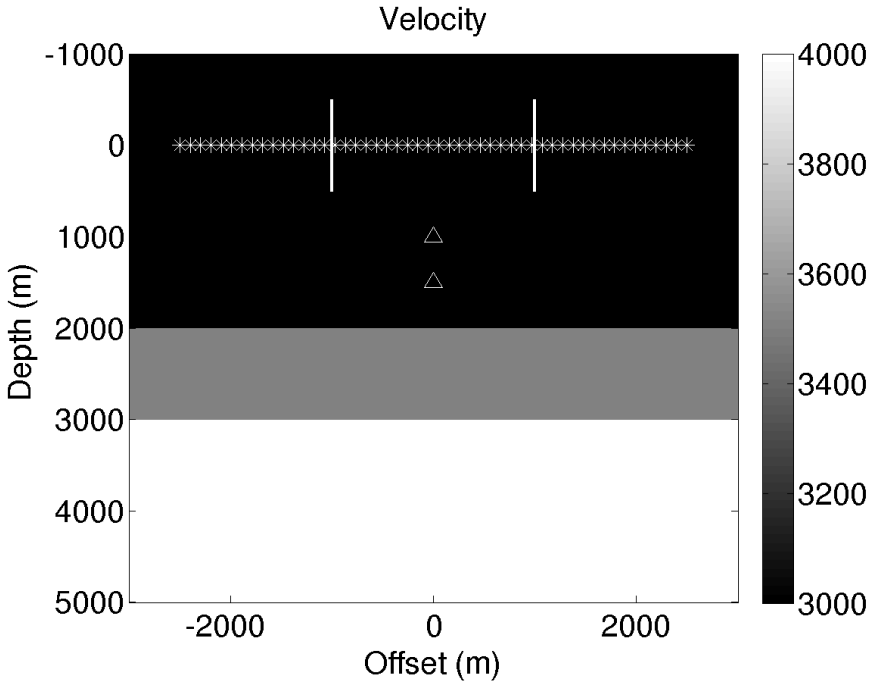

Figure 2: Model with two horizontal reflectors. Velocities are 3000 m/s (top layer), 3500 m/s (middle layer) and 4000 m/s (bottom layer). Stars represent source locations and triangles denote the locations of receivers. All the sources were used in Figure 3. Sources inside two vertical lines were omitted in Figure 5.

If the ideal assumptions are met, the stack should be a bandlimited version of the Green's function. Because our model only contains surface sources and not a completely enclosed contour, the final stack contains artifacts. Notice that the apparent stationary phase (or flattening of the events) at the edges of the correlogram (Figure 3c), particularly at time lags of about 0.05 s, produce large, specious early events in the final stack (Figure 3d). These effects would be eliminated with full source coverage. However, we still observe that the formation reflections, at about 0.5 s and 1.1 s, are recovered very well.

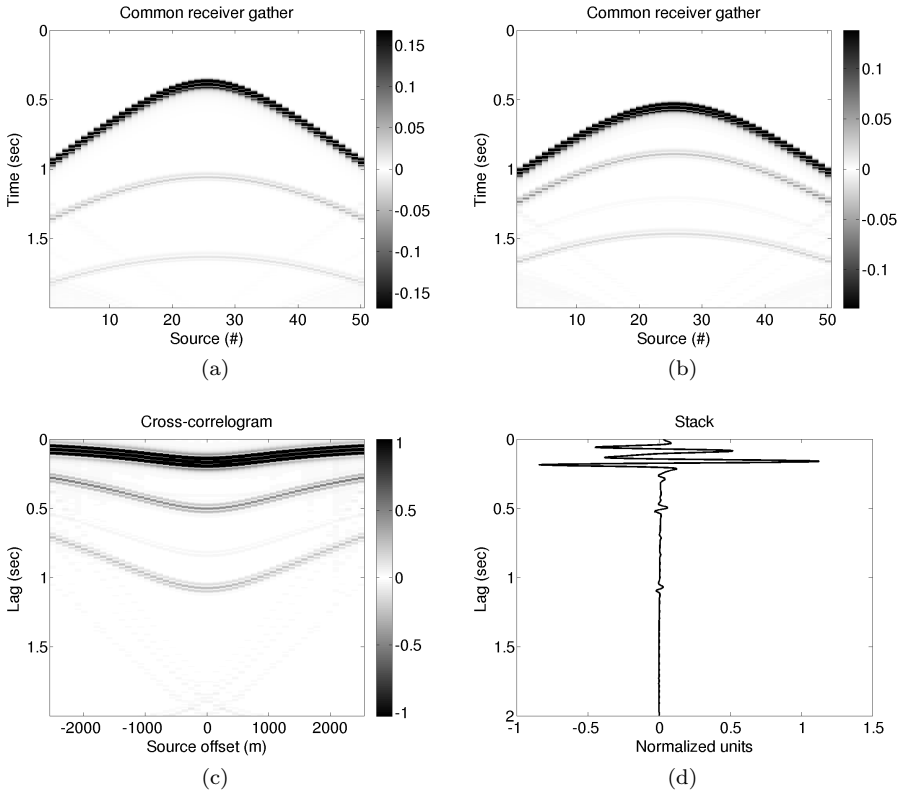

Figure 3: The common receiver gathers for the model with two flat reflectors (Figure 2) for (a) the shallow receiver, and (b) the deep receiver. A direct wave is followed by two reflectors in each case. (c) Their correlogram with only positive lags shown. Correlations of direct waves (at about 0.1 s) dominate the gather. Correlations of direct and reflected waves (at about 0.5 and 1.1 s) have lower amplitudes. (d) The stack of the correlogram showing that the arrival times of the events correspond to stationary phase points in the correlogram.

2.2 Effects of limited source aperture

The desired outcome of stacking the correlations is to isolate and recover energy from each specular reflection point which was "properly" illuminated by the set of physical sources. The specular reflection is properly illuminated when the energy ray path from one of the physical sources passes through the virtual source, is reflected back from the formation boundary at the specular reflection location, and arrives at the virtual receiver. Most of the energy from the set of physical sources will in fact not generate useful interferometric reflections since their ray paths passing through the virtual source will be reflected from the formation boundary in other directions away from the virtual receiver [4]. The special source location that guarantees the proper illumination produces a stationary phase point on its corresponding trace in the set of cross-correlated traces. When a source is not located at this special position, the cross-correlated events from this formation boundary will be at earlier time lags than the stationary phase point. When we have compete source coverage and these correlated traces are stacked together, their contributions will cancel each other out leaving only the stationary phase contribution from the special source location.

If the sources are spaced too far apart, e.g., using only the shots spaced 500 m apart in Figure 2, events in the correlogram will not appear continuous between the traces and would thus be spatially undersampled (Figure 4a). Without a complete set of source illumination points, there will be gaps between the events in the traces of the correlogram, and the subsequent stack of the correlations will leave "ringing" aliased noise in the stack, at earlier times than the stationary phase points. In this case, the proper reflections from the formation boundaries layers will likely be obscured by these noise events. Thus simple stacking of the traces to implement interferometric redatuming in this case breaks down and is unusable.

When there are large gaps in source coverage, e.g., when lakes or platforms restrict source access, entire sections of the correlogram may be missing. To demonstrate, we omit all of the sources in Figure 2, between the vertical lines. The omission of these shots removes the stationary phase points in the correlogram (Figure 5a), and the stack produces a trace (Figure 5b), where each event is specious and erroneous. These specious events are edge effects that would have stacked out, if there had been complete source coverage. Thus these apparent arrivals are non-physical and solely a result of insufficient source coverage.

Whatever the cause of the exact deficiency in source illumination, simply stacking a correlogram might not produce an accurate virtual trace.

2.3 Correlogram event moveout

While we could consider any arbitrarily shaped formation boundary, we limit our analysis to a set of simple point diffractors and flat or dipping reflectors. Each of these boundaries exhibits itself as an event with a different moveout shape across the traces in a correlogram gather. To simplify presenting the equations, we assume a vertical borehole, as shown in Figure 1, but the concepts can

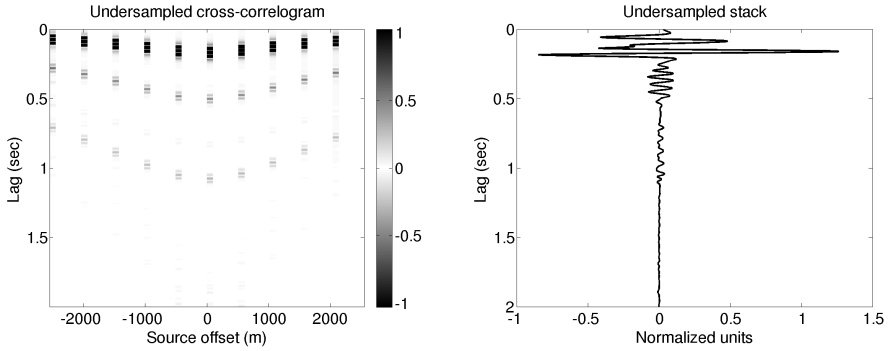

(a) (b)

Figure 4: (a) Correlogram computed for the spatially undersampled model from Figure 2. Note the discontinuous events; (b) Stacking the undersampled correlogram results in "ringing noise" due to non-cancellation of steep parts of the correlogram.

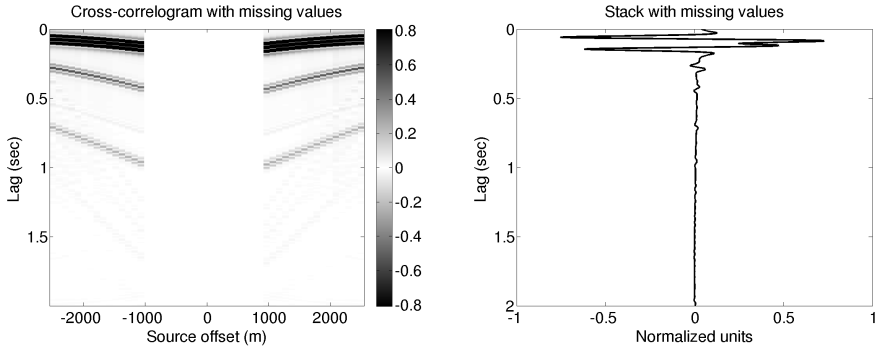

(a) (b)

Figure 5: (a) Correlogram computed for the model from Figure 2 with sources in the middle of the model between the vertical lines removed. Note the absence of stationary phase points; (b) The stack contains only non-physical events.

be extended to deviated and horizontal wells and thus applied to any receiver geometry.

2.3.1 Point diffractor

Suppose that there is a single point diffractor inside the medium, and the surface shots and down-hole receivers are as previously described. Each common receiver gather will record a transmitted (direct) wave and a scattered wave from the point diffractor (for uniformity of notation the scattered wave will always be denoted R for "reflection" whether it is an actual reflection or a diffraction). The correlogram will therefore contain four events resulting from pair-wise cross-correlation of each of the two events in one gather with the two events in another gather. Specifically we will have the direct wave correlated with the direct wave (DD), the direct wave at the VS correlated with the scattered wave at the VR (DR), the scattered wave at the VS correlated with the direct wave at the VR (RD), and the scattered wave correlated with the scattered wave (RR). For a medium with a constant velocity, their moveouts, τ, are given by

$$\tau_{\mathrm{DD}} = \frac{\sqrt{x_{\mathrm{s}}^2 + z_{\mathrm{r},2}^2}}{v} - \frac{\sqrt{x_{\mathrm{s}}^2 + z_{\mathrm{r},1}^2}}{v}; \tag{2a}$$

$$\tau_{\mathrm{DR}} = \frac{\sqrt{(x_{\mathrm{s}} - x_{\mathrm{d}})^2 + z_{\mathrm{d}}^2} + \sqrt{x_{\mathrm{d}}^2 + (z_{\mathrm{r},2} - z_{\mathrm{d}})^2}}{v} - \frac{\sqrt{x_{\mathrm{s}}^2 + z_{\mathrm{r},1}^2}}{v}; \tag{2b}$$

$$\tau_{\mathrm{RD}} = \frac{\sqrt{(x_{\mathrm{s}} - x_{\mathrm{d}})^2 + z_{\mathrm{d}}^2} + \sqrt{x_{\mathrm{d}}^2 + (z_{\mathrm{r},1} - z_{\mathrm{d}})^2}}{v} - \frac{\sqrt{x_{\mathrm{s}}^2 + z_{\mathrm{r},2}^2}}{v}; \tag{2c}$$

$$\tau_{\mathrm{RR}} = \frac{\sqrt{x_{\mathrm{d}}^2 + (z_{\mathrm{r},2} - z_{\mathrm{d}})^2}}{v} - \frac{\sqrt{x_{\mathrm{d}}^2 + (z_{\mathrm{r},1} - z_{\mathrm{d}})^2}}{v}. \tag{2d}$$

2.3.2 Flat reflector

Suppose now that the medium contains a flat reflector at a depth z_ℓ, instead of a diffractor. As in the previous case, the correlogram will have four different events: the direct wave correlated with the direct wave (DD), the direct wave at the VS correlated with the reflected wave at the VR (DR), the reflected wave at the VS correlated with the direct wave at the VR (RD), and the reflected wave correlated with the reflected wave (RR). Their moveouts are given by:

$$\tau_{\mathrm{DD}} = \frac{\sqrt{x_{\mathrm{s}}^2 + z_{\mathrm{r},2}^2}}{v} - \frac{\sqrt{x_{\mathrm{s}}^2 + z_{\mathrm{r},1}^2}}{v}; \tag{3a}$$

$$\tau_{\mathrm{DR}} = \frac{\sqrt{x_{\mathrm{s}}^2 + 4z_\ell^2 - 4z_\ell z_2 + z_{\mathrm{r},2}^2}}{v} - \frac{\sqrt{x_{\mathrm{s}}^2 + z_{\mathrm{r},1}^2}}{v}; \tag{3b}$$

$$\tau_{\mathrm{RD}} = \frac{\sqrt{x_{\mathrm{s}}^2 + z_{\mathrm{r},2}^2}}{v} - \frac{\sqrt{x_{\mathrm{s}}^2 + 4z_\ell^2 - 4z_\ell z_1 + z_{\mathrm{r},1}^2}}{v}; \tag{3c}$$

$$\tau_{\mathrm{RR}} = \frac{\sqrt{x_{\mathrm{s}}^2 + 4z_\ell^2 - 4z_\ell z_{\mathrm{r},2} + z_{\mathrm{r},2}^2}}{v} - \frac{\sqrt{x_{\mathrm{s}}^2 + 4z_\ell^2 - 4z_\ell z_{\mathrm{r},1} + z_{\mathrm{r},1}^2}}{v}. \tag{3d}$$

2.3.3 Dipping reflector

Next we look at the moveout for a dipping reflector. Suppose a planar reflector passes through a point (x_ℓ, z_ℓ) and has a dip θ_ℓ. Then we can write the formulas for event moveouts inside a correlogram as in Equation (2), where $\boldsymbol{x}_{\mathrm{d}}$ is now a point that depends on $\boldsymbol{x}_{\mathrm{s}}$ and $\boldsymbol{x}_{\mathrm{r}}$:

$$\begin{aligned} x_{\mathrm{d}} &= x_\ell + x' \cos\theta_\ell \\ z_{\mathrm{d}} &= z_\ell + x' \sin\theta_\ell \end{aligned}, \tag{4a}$$

where

$$\begin{aligned} x' = -x_\ell \cos\theta_\ell + (z_{\mathrm{r}} - z_\ell)\sin\theta_\ell \\ + \frac{(x_\ell \sin\theta_\ell + (z_{\mathrm{r}} - z_\ell)\cos\theta_\ell)((x_{\mathrm{s}} - x_\ell)\cos\theta_\ell - z_\ell \sin\theta_\ell + x_\ell \cos\theta_\ell + (z_\ell - z_{\mathrm{r}})\sin\theta_\ell))}{(x_\ell - x_{\mathrm{s}})\sin\theta_\ell - z_\ell \cos\theta_\ell + x_\ell \sin\theta_\ell + (z_{\mathrm{r}} - z_\ell)\cos\theta_\ell}. \end{aligned} \tag{4b}$$

3 Semblance moveout analysis

3.1 Motivation

We see from the last section that the moveout from any point diffractor or dipping reflector has a distinct and deterministic moveout. By analyzing the moveout of each event in a correlogram, we can infer the subsurface structures that have produced them. Recently, we developed velocity analysis tools to study events in seismic interferometric correlograms to study the moveout of point scatterers and dipping reflectors [13, 14, 15]. In these analyses, the differential moveout of the events in the correlogram are analyzed using a semblance statistic. In a similar approach, [16] analyzed model data with a single flat layer to recover its velocity. Here we expand these type of analyses to be able to enhance desired events, as well as remove artifacts and unwanted events before stacking the traces in a correlogram gather. Notice that we do not have to have the exact moveout of an event to improve it or filter it out. As long as the moveout function is approximately correct, we can perform specific trace operations, like median filtering, with beneficial effects.

Our analysis is based on a natural extension of the semblance functional, which is a measure of coherence of the traces in the correlogram gather along a given moveout. Values of the semblance close to one will indicate that the moveout is correctly estimated, while erroneous moveouts will result in a semblance value close to zero.

3.2 Semblance for constant medium

Suppose we have a correlogram $C(\boldsymbol{x}_{\rm s}, \tau)$ parameterized by shot location (offset), $\boldsymbol{x}_{\rm s}$, and correlation lag, τ. From a given velocity model, we can predict the arrival times, $\tau(\boldsymbol{x}_{\rm s}; z_\ell, \theta_\ell, v)$, of a reflection (or diffraction) event in the traces of the correlogram. To describe τ for a constant velocity model, we use Equation (2b) for a diffraction, Equation (3b) for a horizontal reflector, and Equations (4) for a dipping reflector. The *depth-velocity* semblance is then defined as follows:

$$S_{\rm depth}(z_\ell, \theta_\ell, v) = \frac{\displaystyle\int_{-T/2}^{T/2} \left[\int_{\mathscr{S}} C\big(\boldsymbol{x}_{\rm s}, \tau(\boldsymbol{x}_{\rm s}; z_\ell, \theta_\ell, v) + t\big)\, d\boldsymbol{x}_{\rm s} \right]^2 dt}{|\mathscr{S}| \displaystyle\int_{-T/2}^{T/2} \int_{\mathscr{S}} C^2\big(\boldsymbol{x}_{\rm s}, \tau(\boldsymbol{x}_{\rm s}; z_\ell, \theta_\ell, v) + t\big)\, d\boldsymbol{x}_{\rm s}\, dt}. \tag{5}$$

We have chosen the time window integration length to be the period of the source wavelet, T. A larger time window will achieve greater stability at the expense of resolution.

As with a conventional NMO velocity analysis, high semblance values using Equation (5) to analyze a correlogram will identify events with moveouts matching the predictions given by Equations (2, 3 or 4). Because our goal is to directly identify reflection events in the correlogram, it is convenient to convert the parameterization of the semblance analysis from depth and velocity to time and velocity. So we define $t = T_{\theta_\ell, v}(z_\ell)$ as the reflection time from the virtual source (VS) to the possible reflector and back to the virtual receiver (VR). We then define the *time-velocity* semblance as

$$S_{\rm time}(t, \theta_\ell, v) = S_{\rm depth}\Big(T^{-1}_{\theta_\ell, v}(t), \theta_\ell, v\Big), \tag{6}$$

where $T^{-1}_{\theta_\ell, v}(t)$ provides a mapping between z_ℓ and t. Thus the transform only stretches the depth axis back to the time lag axis in the correlogram. This allows us to directly map the arrival time lag of the event in the semblance analysis to its stationary phase point time lag in the correlogram gather. Because we perform the semblance stack along the predicted arrivals for a modeled reflection type, either a dipping boundary or a diffraction, we reduce the aliasing created by acquisition gaps source coverage. The high semblance values will provide time lag, dip and velocity triples for possible events in the correlogram gather. This information can be used to either enhance or filter out these events before the traces are stacked to create the redatumed trace.

3.3 Semblance for multilayered medium

The moveout curves (Equations 2, 3 and 4) we used in the semblance analysis assume constant velocity in the medium. In most practical cases this assumption is not valid and so the simplified analysis does not accurately describe the

moveout for a dipping layer velocity medium. The final stacked and redatumed trace will be independent of the velocity above VS. However, before stacking, the moveout in the correlogram will be a function of the velocities encountered by the rays all the way from the surface down to the reflector. We can estimate the velocity above VS and VR using the first break arrival times of the common receiver gathers (e.g., as in Figures 3a and 3b) before correlation. Therefore, we seek to determine the velocity and dip of reflectors below VR. To simplify our analysis we make a straight ray assumption, as shown in Figure 6. The travel times will be computed along straight rays on two paths: 1) from the source to VS, and 2) from the source to the dipping reflector and back to VR.

A dipping layer is shown bounded by two solid lines near the bottom of Figure 6. The reflected ray is shown starting at the source, bouncing off the bottom of the dipping bed, and returning to VR. We draw two dashed lines through VS and VR, each parallel to the dipping reflector. These dashed lines will intersect the reflected ray at points A and B, respectively. Assuming all layers in the medium are parallel, the propagation of the wave in the medium below the line from the point B to the reflector and then to VR is described in terms of the velocity, v, we seek. It is an RMS average of the interval velocities of the layers encountered by the ray below VR. So we modify τ in the semblance analysis (Equation 5 and 6) to use the first break derived velocities, v_{VS}, from the source to VS and v_{VR}, from the source to VR and vary v, the effective velocity below the VS and VR. Ultimately we create a cube of semblances corresponding to a range of dips and velocities for each time in the correlogram. High semblance values reveal events with moveouts aligning with the scanned velocities and dips.

The semblance analysis for the two flat reflectors model in Figure 2, is shown in Figure 7. Here we show the slice of the semblance cube for zero dip ($\theta_\ell = 0$) and vary the velocity and time. The maximum semblance peaks show at time lags 0.5 and 1.1 s, which corresponds to the stationary phase points in Figure 3c.

The corresponding semblance analysis for the two layer dipping model is shown in Figure 8. As before, we selected from the semblance cube the results for the correct dip, $\theta_\ell = 30\,^\circ$, and scanning a range of velocities and time on the correlogram. The semblance analysis for this model shows the stationary phase points at about 1.0 and 1.6 s with different apparent velocities than the flat layer case.

3.4 Semblance for diffractors

We next modify the semblance analysis to track diffraction moveout described in Equation (2b). We apply this analysis to a model with two horizontal boundaries and a single diffractor as described in Figure 9a. The correlogram in Figure 9b shows four events: the direct wave, the two horizontal reflectors and the diffracted event. We can clearly see that the diffraction event is skewed and not symmetric about the zero source offset line making its moveout on the correlogram quite distinctive from the flat reflections. Figure 9c shows the

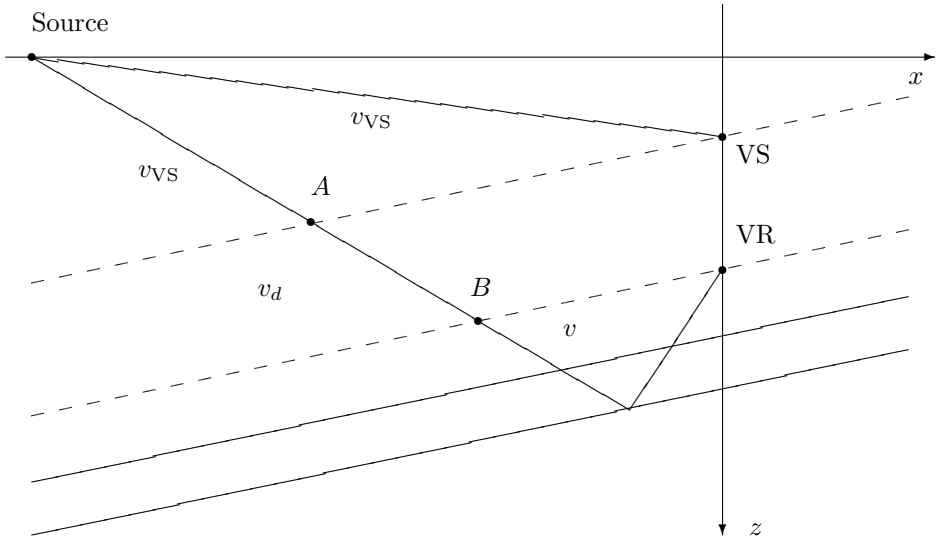

Figure 6: Direct and reflected rays in a medium with dipping layers. The velocity between Source and A is recovered from the first break at VS. The velocity, v_d, between A and B is a combination of the VS and VR velocities. The deep velocity v along the reflected ray from B to VR is to be determined with the semblance analysis.

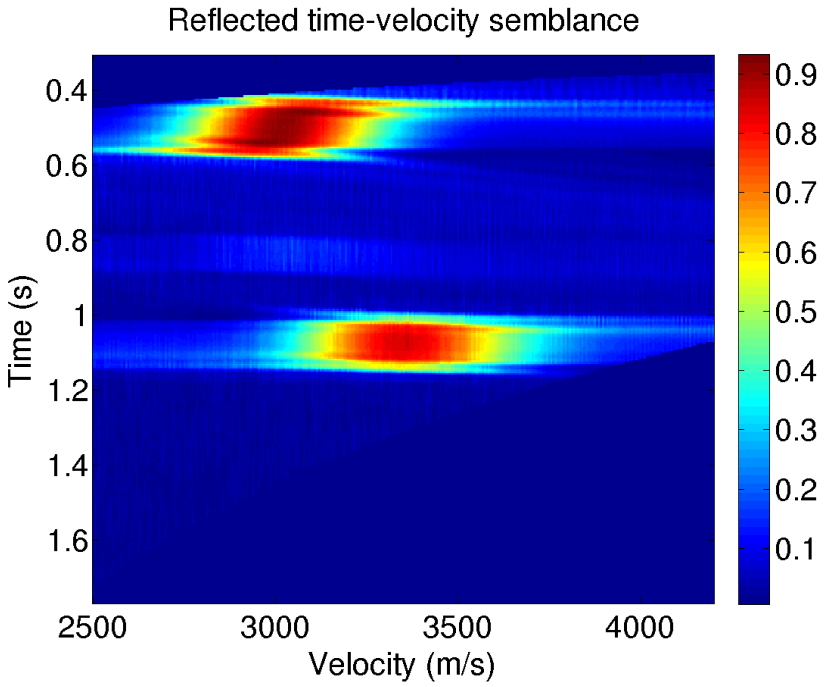

Figure 7: Semblance analysis searching for horizontal reflectors computed for the correlogram in Figure 3c. The two semblance peaks match the lag times (0.5 s and 1.1 s) of the stationary phase points in the correlogram. Their corresponding velocities (3000 m/s and 3400 m/s) are the RMS velocities between VR and each reflector.

result of the semblance analysis using the diffraction moveout. The diffraction effect stands out with an arrival lag time of about 1 s. The horizontal reflectors are not present in the analysis. For comparison, Figure 9d shows the semblance analysis using the flat layer moveout function. The difracted event is missing on the flat layer semblance analysis. We have shown that these semblance analyses are capable of distinguishing between reflected and diffracted events in a correlogram gather.

4 Filtering correlograms

To demonstrate the potential value of the semblance analysis, we examine the stacking process for the correlograms corresponding to the two layer model (Figure 2) and the two layer model with a diffractor (Figure 9a). Figure 10 shows close-ups around the reflection events in the correlograms for (a) the two layer model with a diffractor and (e) the two layer model. For purposes

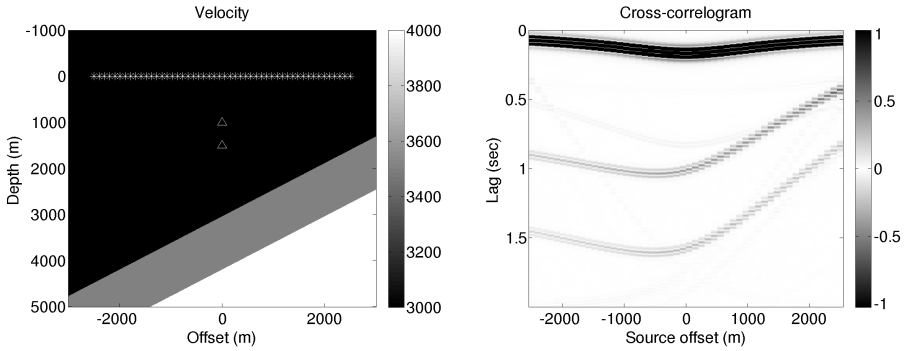

(a)

(b)

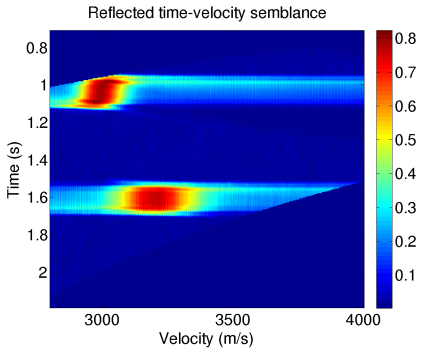

(c)

Figure 8: (a) Model with two reflectors dipping at 30 ° with velocities 3000 m/s (top layer), 3500 m/s (middle layer) and 4000 m/s (bottom layer); (b) Correlogram with a direct event (0.1 s) and two reflected events (1.0 s and 1.6 s); (c) Reflected semblance computed for dip of 30 °.

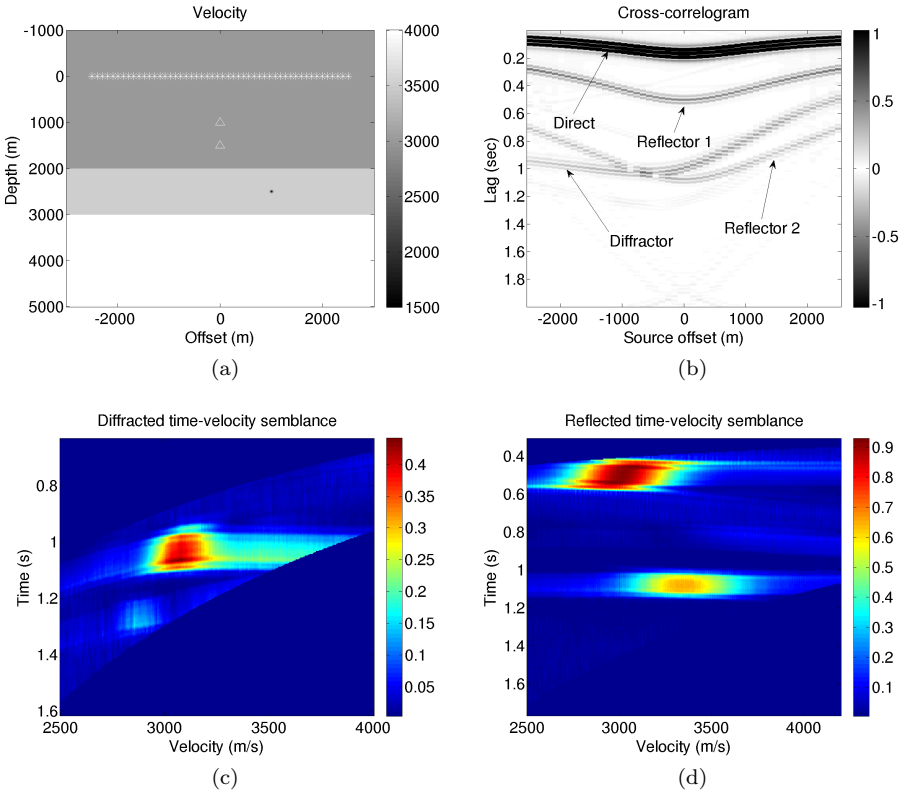

Figure 9: (a) Model with two flat reflectors and a point diffractor, with layer velocities 3000 m/s (top layer), 3500 m/s (middle layer) and 4000 m/s (bottom layer); (b) The correlogram containing an additional diffracted event; (c) Semblance computed using *diffracted* moveouts shows one large event; (d) Semblance computed using *reflected* moveouts shows two events.

of illustration, our aim is to remove the diffration event from the correlogram before stacking and thus enhance the horizontal reflectors.

Performing a brute stack of the traces in a correlogram gather can introduce edge effects. Figure 11a shows a close up of a simple stack of the correlogram (in Figure 10a) for the two layer plus diffractor model. Because we do not have complete source coverage around the receivers, we introduce edge effects visible for every event at the edge of the correlogram. This is particularly obvious at 0.7 and 0.9 s. Applying a simple taper (weighting function) before stacking that de-emphasizes the far offset traces, we obtain an enhanced stack shown in Figure 11b. The edge effects have been reduced. Our goal is to obtain a match with the tapered stack (Figure 11d) of the correlogram for the two layer model. Comparing these two traces we see that the second layer event starting at about 1.02 s (in Figure 11d) is contaminated with a precursor from the diffraction event that starts at about 0.95 s in Figure 11b.

We use the predicted velocity moveout of the diffraction from the picked semblance analysis in Figure 9c to align by time shifting the correlogram in Figure 10a. The flattened correlogram is shown in Figure 10b, where the diffraction event is now at about 0.8 s. (Notice that it is not exactly flat due to the straight ray approximation used.) Next a simple eleven trace, running mean is subtracted from each trace and the results are shown in Figure 10c. This filtering process removes events which are locally time consistent in the flattened correlogram. We see the diffraction event has been successfully removed. Then the filtered correlogram has the diffraction moveout re-applied, resulting in Figure 10d. We see that our simple filtering process has also removed some of the tails of the right hand side of the second reflection event, between traces 40 and 50, and times 0.7 to 0.9 s. These portions ended up being removed since its moveout away from the stationary phase is nearly parallel with the diffractor moveout. (This can be seen in Figure 10a for traces 40 and above.) Since these portions are far from the stationary phase, they are unimportant and may be omitted if they are removed smoothly and without large trace to trace changes in amplitudes. The tapered stack of the final filtered correlogram is shown in Figure 11c. We obtain a very good match between the reference two layer stacked trace (Figure 11d) with our filtered trace (Figure 11c).

5 Conclusions

Seismic interferometry involves stacking a correlogram formed from two common receiver gathers. This process assumes idealized conditions rarely met in real geophysical applications. When those assumptions are violated, artifacts may be introduced into the interferometrically redatumed trace. Without proper preconditioning, these artifacts may be indistinguishable from the desired reflections making the final redatumed trace filled with erroneous events. Improving a redatumed trace for a virtual source and receiver pair requires an understanding of the intermediate correlogram and the basic events that comprise it. We have proposed moveout curves for events corresponding to point

diffractors and dipping reflectors. Semblance analysis allows us to distinguish between different events based upon dip, velocity and event type (reflection and diffraction). The estimated moveouts from the semblance analysis can be used to filter the correlograms and consequently improve interferometric stacks.

6 Acknowledgements

This work was supported by the Earth Resources Laboratory Founding Member Consortium and by ConnocoPhillips. The authors would like to thank Stéphane Rodenay, Alison Malcolm, Bongani Machele and Maria Gabriela Melo Silva for many useful joint discussions of this work.

References

[1] Valeri Korneev and Andrey Bakulin. On the fundamentals of the virtual source method. *Geophysics*, 71(3):A13–A17, 2006.

[2] Mark E. Willis, Rongrong Lu, Xander Campman, M. Nafi Toksöz, Yang Zhang, and Maarten V. de Hoop. A novel application of time-reversed acoustics: Salt-dome flank imaging using walkaway VSP surveys. *Geophysics*, 71(2):A7–A11, March–April 2006.

[3] Brian E. Hornby and Jianhua Yu. Interferometric imaging of a salt flank using walkaway VSP data. *Leading Edge*, 26(6):760–763, June 2007.

[4] Ronrong Lu, Mark E. Willis, Xander Campman, Jonathan Ajo-Franklin, and M. Nafi Toksöz. Redatuming through a salt canopy and target oriented salt-flank imaging. *Geophysics*, 73:S63–S71, 2008.

[5] James Rickett and Jon Claerbout. Passive seismic imaging applied to synthetic data. Technical Report 92, Stanford Exploration Project, 1996.

[6] Arnaud Derode, Eric Larose, Michel Campillo, and Mathias Fink. How to estimate the Green's function of a heterogeneous medium between two passive sensors? Application to acoustic waves. *Applied Physics Letters*, 83(15):3054–3056, 2003.

[7] Andrey Bakulin and Rodney Calvert. Virtual source: new method for imaging and 4D below complex overburden. *74th Annual International Meeting, SEG, Expanded Abstracts*, pages 2477–2480, 2004.

[8] Gerard T. Schuster, J. Yu, J. Sheng, and J. Rickett. Interferometric/daylight seismic imaging. *Geophysical Journal International*, 157(2):838–852, May 2004.

[9] Kees Wapenaar, Jacob T. Fokkema, and Roel Snieder. Retrieving the Green's function in an open system by cross correlation: a comparison of

approaches. *Journal of the Acoustical Society of America*, 118(5):2783–2786, November 2005.

[10] Kurang Mehta, Roel Snieder, Rodney Calvert, and Jonathan Sheiman. Acquisition geometry requirements for generating virtual-source data. *The Leading Edge*, 27(5):620–629, May 2008.

[11] Kees Wapenaar. Retrieving the elastodynamic Green's function of an arbitrary inhomogeneous medium by cross correlation. *Physical Review Letters*, 93(25):254301–1–4, 2004.

[12] Gerard T. Schuster and Min Zhou. A theoretical overview of model-based and correlation-based redatuming methods. *Geophysics*, 71(4):S1103–S1110, 2006.

[13] Oleg V. Poliannikov and Mark E. Willis. Improved Green's functions from seismic interferometry. Technical report, Earth Resources Laboratory, Department of EAPS, MIT, Cambridge, MA, June 2008.

[14] Oleg V. Poliannikov, Mark E. Willis, and Bongani Machele. Interferometric correlogram-space analysis. Technical report, Earth Resources Laboratory, Department of EAPS, MIT, Cambridge, MA, June 2009.

[15] Oleg V. Poliannikov, Mark E. Willis, and Bongani Machele. Interferometric correlogram-space analysis. *Eos Trans. AGU*, 90(52), 2009. Fall Meet. Suppl., Abstract S42A-05.

[16] Simon King, Andrew Curtis, and Travis Poole. Interferometric velocity analysis using physical and non-physical energy. *79th Annual International Meeting, SEG, Expanded Abstracts*, 2009.

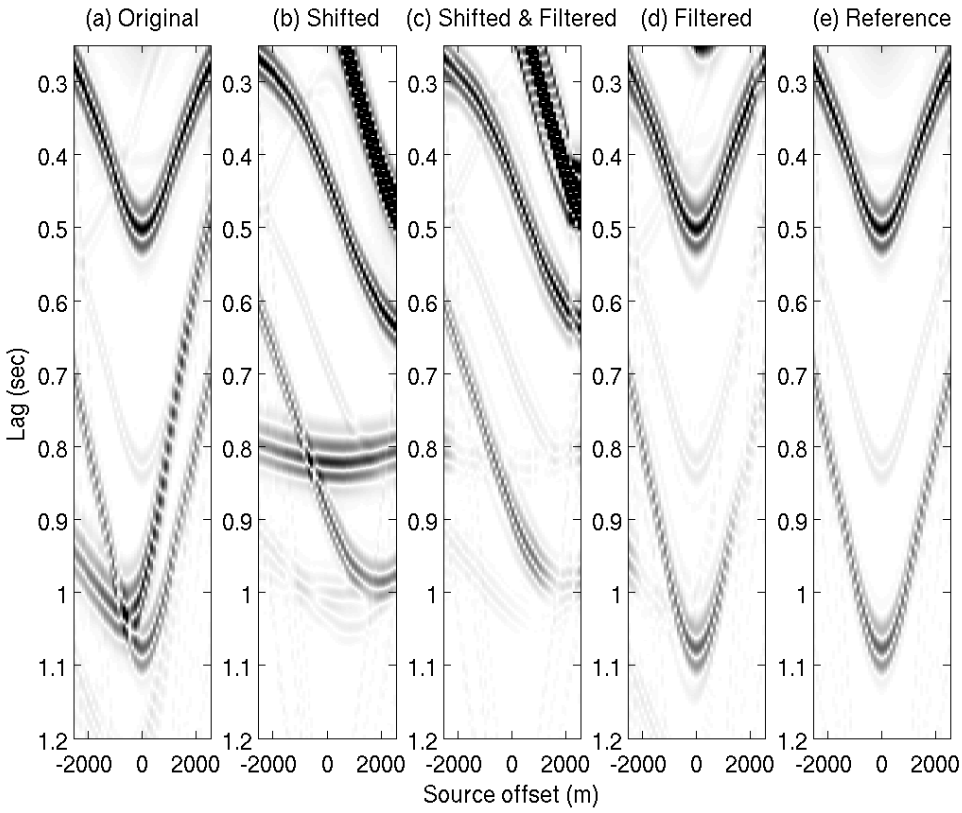

Figure 10: Close-up of correlograms for the (a) two layer model with diffractor in Figure 9a, (b) time shifted version of correlogram to flatten diffractor now at about 0.8 s, (c) the mean filtered version of the time shifted correlogram, (d) the final filtered version shifted back to proper time where we see that the diffrator has been removed, and (e) the reference two layer model in Figure 2 which we are trying to simulate.

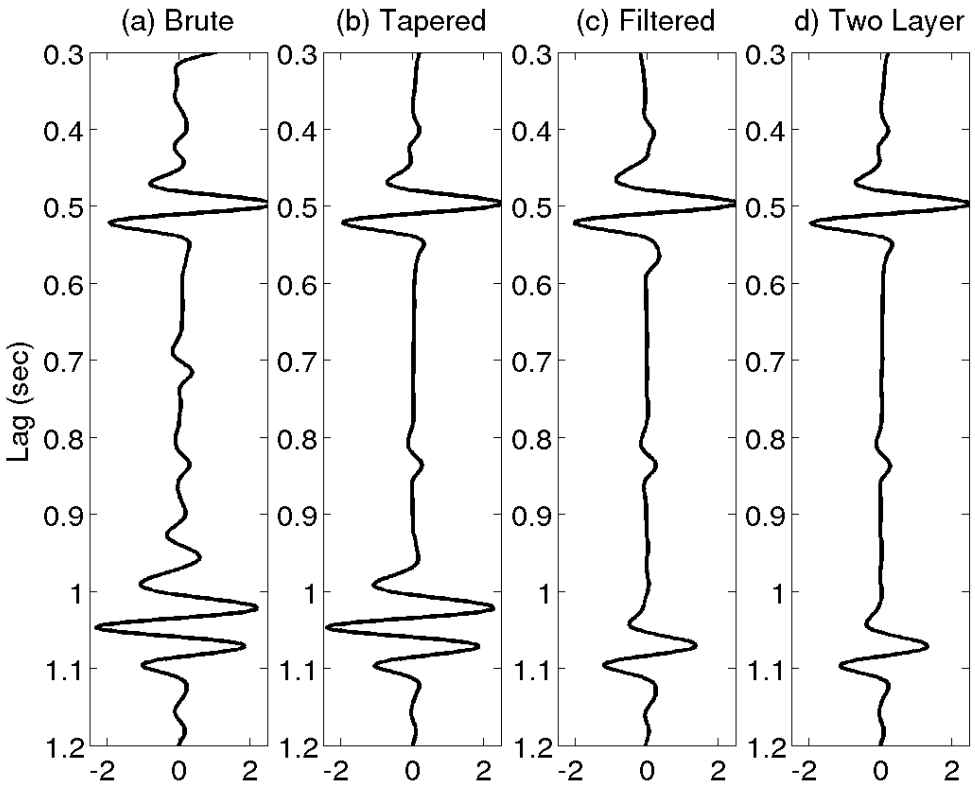

Figure 11: Stacked correlograms for (a) brute stack of Figure 10b, (b) tapered stack of Figure 10b, (c) filtered and tapered stack of Figure 10b, and (d) tapered stack of the two layered model in Figure 10a. Note the good match between the filtered version c and the two layer reference trace, d.